

Let There be Direction in Hypergraph Neural Networks

Anonymous authors

Paper under double-blind review

Abstract

Hypergraphs are a powerful abstraction for modeling high-order interactions between a set of entities of interest and have been attracting a growing interest in the graph-learning literature. In particular, directed hypergraphs are crucial in their capability of representing real-world phenomena involving group relations where two sets of elements affect one another in an asymmetric way. Despite such a vast potential, an established, principled solution to tackle graph-learning tasks on directed hypergraphs is still lacking. For this reason, in this paper we introduce the *Generalized Directed Hypergraph Neural Network* (GeDi-HNN), the first spectral-based Hypergraph Neural Network (HNN) capable of seamlessly handling hypergraphs featuring both directed and undirected hyperedges. GeDi-HNN relies on a graph-convolution operator which is built on top of a novel complex-valued Hermitian matrix which we introduce in this paper: the *Generalized Directed Laplacian* \tilde{L}_N . We prove that \tilde{L}_N generalizes many previously-proposed Laplacian matrices to directed hypergraphs while enjoying several desirable spectral properties. Extensive computational experiments against state-of-the-art methods on real-world and synthetically-generated datasets demonstrate the efficacy of our proposed HNN. Thanks to effectively leveraging the directional information contained in these datasets, GeDi-HNN achieves a relative-percentage-difference improvement of 7% on average (with a maximum improvement of 23.19%) on the real-world datasets and of 65.3% on average on the synthetic ones.

1 Introduction

In recent years, ground-breaking research in the graph-learning literature has been prompted by seminal works on Graph Neural Networks (GNNs) such as (Scarselli et al., 2009; Micheli, 2009; Li et al., 2016; Kipf and Welling, 2017; Veličković et al., 2018). Since representing a set of complex relationships solely through undirected or directed graphs can prove too restrictive in many real-world scenarios, generalizations to graphs allowing for higher-order (group) relationships, i.e., hypergraphs, have been considered. Hypergraphs generalize the notion of a graph to the case where an edge (a hyperedge) can connect an arbitrary number of nodes, thus allowing to capture not just pairwise (dyadic) relationships but also group-wise (polyadic) dynamics (Schaub et al., 2021). This has led to a new stream of research devoted to the investigation of Hypergraph Neural Networks (HNNs) (Feng et al., 2019; Chien et al., 2021; Huang and Yang, 2021; Wang et al., 2023a;b).

While most of the literature on HNNs has focused on undirected hypergraphs, many real-world phenomena such as chemical reactions are naturally modeled on hypergraphs whose hyperedges have a notion of direction. Despite this, the directed case has been addressed only sporadically, and often only in application-specific scenarios such as traffic forecasting (Luo et al., 2022) and music recommendation (La Gatta et al., 2022). To the best of our knowledge, a general solution based on a convolution operator which is solidly grounded in spectral graph theory while not being problem-dependent is missing. We aim at bridging such a gap.

In this paper, we introduce the *Generalized-Directed Hypergraph Neural Network* (GeDi-HNN), the first spectral-based HNN capable of seamlessly handling hypergraphs featuring both directed and undirected hyperedges. GeDi-HNN relies on a graph-convolution operator which is built on top of a novel Hermitian Laplacian matrix which we introduce in this paper: the *Generalized Directed Laplacian* \tilde{L}_N . \tilde{L}_N generalizes various Laplacian matrices: the one proposed in Zhou et al. (2006) and used in Feng et al. (2019) for

undirected hypergraphs, the Sign-Magnetic Laplacian proposed for directed graphs in (Fiorini et al., 2023), and the classical Laplacian matrix (Chung and Graham, 1997) used for undirected graphs.

Main Contributions of the Work

- We extend the literature on spectral-based HNNs by introducing GeDi-HNN, the first spectral HNN capable of handling hypergraphs with both directed and undirected hyperedges.
- We introduce the *Generalized Directed Laplacian* matrix \vec{L}_N ; we prove that it enjoys several desirable properties, among which admitting an eigenvalue decomposition, and that it generalizes many existing Laplacian matrices.
- Compared to state-of-the-art methods, GeDi-HNN achieves a relative-percentage-difference improvement of 7% on average (with a maximum improvement of 23.19%) on the real-world datasets and of 65.3% on average on the synthetic ones. This demonstrates its efficacy in extracting and utilizing the information encoded in the hyperedge directions.

The paper is organized as follows. Preliminaries and previous works are summarized in Section 2. \vec{L}_N is introduced in Section 3, along with its properties. Section 4 provides an overview of GeDi-HNN’s architecture, which is built upon \vec{L}_N . Experimental results are reported in Section 5. Conclusions are drawn in Section 6. The proofs of our theorems and additional details are provided in the Appendix.

2 Preliminaries and Previous Work

Undirected and Directed Hypergraphs

A hypergraph is an ordered pair $\mathcal{H} = (V, E)$, with $n := |V|$ and $m := |E|$, where V is the set of vertices (or nodes) and $E \subseteq 2^V \setminus \{\emptyset\}$ is the (nonempty) set of hyperedges. The hyperedge weights are stored in the diagonal matrix $W \in \mathbb{R}^{m \times m}$. The vertex and hyperedge degrees are defined as $d_u = \sum_{e \in E: u \in e} |w_e|$ for $u \in V$ and $\delta_e = |e|$ for $e \in E$ and are stored in two diagonal matrices $D_v \in \mathbb{R}^{n \times n}$ and $D_e \in \mathbb{R}^{m \times m}$. Hypergraphs where $\delta(e) = k$ for some $k \in \mathbb{N}$ for all $e \in E$ are called k -uniform. Graphs are 2-uniform hypergraphs. Following Gallo et al. (1993), we define a directed hypergraph as a hypergraph where each edge $e \in E$ is partitioned in a *head set* $H(e)$ and a *tail set* $T(e)$. If $T(e)$ is empty, e is an undirected edge.

Graph Fourier Transform and Graph Convolutions

Let \mathcal{L} be a generic Laplacian matrix of a given 2-uniform hypergraph \mathcal{H} which embeds its topology. We assume that \mathcal{L} admits an eigenvalue decomposition $\mathcal{L} = U\Lambda U^*$, with $U \in \mathbb{C}^{n \times n}$, U^* is the conjugate transpose of U , and $\Lambda \in \mathbb{R}^{n \times n}$ is a diagonal matrix. Let $x \in \mathbb{C}^n$ be a *graph signal*, i.e., a function $x : V \rightarrow \mathbb{C}$ whose domain coincides with the vertices of \mathcal{H} . Following Shuman et al. (2013), we call $\hat{x} = \mathcal{F}(x) = U^*x$ the *graph Fourier transform* of x and $\mathcal{F}^{-1}(\hat{x}) = U\hat{x}$ its inverse transform. The eigenvectors u_1, \dots, u_n (columns of U) act as Fourier modes and the eigenvalues $\lambda_1, \dots, \lambda_n$ (on the diagonal of Λ) as Fourier frequencies. The convolution $y \circledast x$ between x and another graph signal $y \in \mathbb{C}^n$ (taking the role of a *filter*) has a natural construction in the frequency space, where it is defined as $y \circledast x = U \text{diag}(U^*y)U^*x$. Letting $\hat{Y} := U\hat{G}U^*$ with $\hat{G} := \text{diag}(U^*y)$, we can write $y \circledast x$ in the vertex space as the linear operator $\hat{Y}x$.

In the context of a GNN, there are two drawbacks to learning y explicitly as a *non-parametric filter*: *i)* deriving the eigenvalue decomposition of \mathcal{L} could be computationally too intensive (Kipf and Welling, 2017); *ii)* learning y explicitly would require learning a number of parameters proportional to the input size, which could be inefficient for tasks of high dimension (Defferrard et al., 2016).

For these reasons, it is customary in the GNN literature, see Kipf and Welling (2017) and Defferrard et al. (2016), to work with filters whose graph Fourier transform is a degree- K polynomial function of Λ with a small K . This leads to a so-called *localized filter* thanks to which the output (i.e., filtered) signal at a vertex $u \in V$ is a linear combination of the input signals within a K -hop neighborhood of u (Shuman et al., 2013).

Using either Chebyshev polynomials as done by Hammond et al. (2011) and Kipf and Welling (2017) or power monomials as done by Singh and Chen (2022), with $K = 1$ (as typical in the literature) one obtains a parametric family of linear operators with two (learnable) parameters θ_0 and θ_1 :¹

$$\hat{Y} := \theta_0 I + \theta_1 \mathcal{L}. \quad (1)$$

Discrete Laplacians for Undirected Hypergraphs

In a hypergraph $\mathcal{H} = (V, E)$, the relationship between vertices and hyperedges is classically represented via an incidence matrix B of size $|V| \times |E|$. When \mathcal{H} is undirected, B is defined as:

$$B_{ve} = \begin{cases} 1 & \text{if } v \in e \\ 0 & \text{otherwise} \end{cases} \quad v \in V, e \in E. \quad (2)$$

From B , one can derive Q , the *Signless Laplacian Matrix* Chung and Graham (1997), as well as its normalized counterpart Q_N :

$$Q := BWB^\top \quad Q_N := D_v^{-\frac{1}{2}} B W D_e^{-1} B^\top D_v^{-\frac{1}{2}}. \quad (3)$$

When restricting to undirected graphs (i.e., 2-uniform undirected hypergraphs), an alternative Laplacian matrix, the so-called *Signed Laplacian Matrix*, can be obtained with a similar construction to equation 3. This involves applying an arbitrary orientation to the edges of the graph (i.e., arbitrarily multiplying by -1 exactly one entry per column of B). Calling such a matrix B' , the *Signed Laplacian matrix* L and its normalized counterpart L_N are defined as follows:

$$L := B' W B'^\top \quad L_N := D_v^{-\frac{1}{2}} B' W D_e^{-1} B'^\top D_v^{-\frac{1}{2}}. \quad (4)$$

By utilizing the standard definitions of weighted adjacency matrix $A \in \mathbb{R}^{n \times n}$ where $A_{uv} = w_e$ if $e = \{u, v\} \in E$ and $A_{uv} = 0$ otherwise, for undirected graphs we have:

$$Q = D_v + A \quad L = D_v - A \quad Q_N = I - L_N \quad L_N = I - Q_N. \quad (5)$$

While the definition of L in equation 4 does not extend nicely to general (not 2-uniform) hypergraphs, the definition of L_N in equation 5 does.² A generalization of the *Signed Laplacian* to general undirected hypergraphs which follows $L_N = I - Q_N$ from equation 5 is proposed by Zhou et al. (2006), and reads:³

$$\Delta = I - Q_N. \quad (6)$$

Notably, all the Laplacian matrices we introduced satisfy some key properties: *i*) they are real and symmetric—and thus diagonalizable with real-valued eigenvalues; *ii*) they are positive semi-definite; and *iii*) their normalized versions possess a bounded spectrum.

Discrete Laplacian Matrices for Directed 2-Uniform Hypergraphs

In directed 2-uniform hypergraphs, the presence of edge directions renders the graph asymmetric and none of the previous definitions of the graph Laplacian apply. Indeed, those in equation 3, equation 4, and equation 6 would symmetrize the graph and destroy its directions, while the one in equation 5 would lead to an asymmetric matrix which does not admit an eigenvalue decomposition and, thus, would prevent the application of the graph Fourier transform.

¹Following w.l.o.g. Singh and Chen (2022), we employ the approximation $\hat{G} = \sum_{k=0}^K \theta_k \Lambda^k$, from which we deduce $\hat{Y} x = U \hat{G} U^* x = U (\sum_{k=0}^K \theta_k \Lambda^k) U^* x = \sum_{k=0}^K \theta_k (U \Lambda^k U^*) x = \sum_{k=0}^K \theta_k \mathcal{L}^k x$.

²For instance, the choice of which entries of B should be multiplied by -1 would drastically affect L (rendering the orientation not arbitrary anymore) and L may feature both positive and negative off-diagonal entries, thereby violating $L_N = I - Q_N$ (notice that $Q_N \geq 0$ holds by construction).

³In Zhou et al. (2006), Q_N is called Θ .

The *Magnetic Laplacian* $L^{(q)}$, proposed by Lieb and Loss (1993) in the context of electromagnetic fields and adopted within a spectral GNN by Zhang et al. (2021b;a), is a complex-valued and Hermitian Laplacian matrix. It encodes the directional information of the graph while enjoying an eigenvalue decomposition with a nonnegative, real spectrum. This Laplacian matrix generalizes the Laplacian L defined in equation 5. Letting $A_s := \frac{1}{2}(A + A^\top)$ be the symmetrized version of A and letting $D_s := \text{diag}(A_s e)$, the *Magnetic Laplacian* and its normalized version are defined as follows:

$$L^{(q)} := D_s - H^{(q)} \text{ and } L_N^{(q)} := I - D_s^{-\frac{1}{2}} H^{(q)} D_s^{-\frac{1}{2}}, \text{ with } H^{(q)} := A_s \odot \exp(i 2\pi q (A - A^\top)),$$

where i is the imaginary unit and $q \in [0, 1]$.

The *Sign-Magnetic Laplacian* L^σ is a matrix proposed by Fiorini et al. (2023) which is well-defined also for graphs with negative edge weights and enjoys some extra desirable properties. If $q = \frac{1}{4}$, L^σ and $L^{(q)}$ coincide if the latter is first constructed for an unweighted version of the graph and then multiplied component-wise by A_s . Thus, L^σ is invariant to a positive weight scaling which could otherwise alter the sign pattern of $L^{(q)}$ and, thus, the edge direction. Letting $\bar{D}_s := \text{diag}(|A_s| e)$ and $\text{sign} : \mathbb{R} \rightarrow \{-1, 0, 1\}$ be the component-wise *signum* function, L^σ and its normalized version are defined as follows:

$$L^\sigma := \bar{D}_s - H^\sigma \text{ and } L_N^\sigma := I - \bar{D}_s^{-\frac{1}{2}} H^\sigma \bar{D}_s^{-\frac{1}{2}}, \text{ with } H^\sigma := A_s \odot \left(e^\top - \text{sign}(|A - A^\top|) + i \text{sign}(|A| - |A^\top|) \right).$$

To the best of our knowledge, no extensions of the Laplacian matrix are known for the case of directed hypergraphs which are not 2-uniform. Our paper aims to bridge this gap.

3 The Generalized Directed Laplacian

We now introduce our proposed complex-valued Hermitian Laplacian matrix, which is capable of handling hypergraphs featuring both directed and undirected hyperedges. We also establish some of its key properties. We refer to this matrix as the *Generalized Directed Laplacian*. We define it directly in normalized form as:

$$\vec{L}_N := I - \vec{Q}_N \quad \text{with} \quad \vec{Q}_N := D_v^{-\frac{1}{2}} \vec{B} W D_e^{-1} \vec{B}^* D_v^{-\frac{1}{2}}, \quad (7)$$

where \vec{B} is the following complex-valued incidence matrix:

$$\vec{B}_{ve} = \begin{cases} 1 & \text{if } v \in H(e) \\ -i & \text{if } v \in T(e) \\ 0 & \text{otherwise} \end{cases} \quad v \in V, e \in E. \quad (8)$$

To appreciate how \vec{L}_N encodes the directions of the hypergraph, we analyze its scalar form for a pair of vertices $u, v \in V$:

$$(\vec{L}_N)_{uv} = \begin{cases} 1 - \sum_{e \in E: u \in e} \frac{w_e}{\delta_e} \frac{1}{d_u} & u = v \\ \left(- \sum_{e \in E: u, v \in H(e) \vee u, v \in T(e)} \frac{w_e}{\delta_e} - i \left(\sum_{e \in E: u \in T(e) \wedge v \in H(e)} \frac{w_e}{\delta_e} - \sum_{e \in E: u \in H(e) \wedge v \in T(e)} \frac{w_e}{\delta_e} \right) \right) \frac{1}{\sqrt{d_u}} \frac{1}{\sqrt{d_v}} & u \neq v \end{cases} \quad (9)$$

The pair u, v affects the value of $(\vec{L}_N)_{uv}$ through each hyperedge $e \in E$ where $u, v \in e$. Considering the second line of equation 9, each hyperedge where u, v take both the role of head ($u, v \in H(e)$) or tail ($u, v \in T(e)$) contributes negatively to the real part, $\Re((\vec{L}_N)_{uv})$, by the opposite of its normalized weight ($-w_e/\delta_e$). For undirected hypergraphs, this is the only contribution. Such a behavior is in line with the nature of L_N (equation 4) for undirected graphs and of Δ (equation 6) for undirected hypergraphs. Hyperedges where u, v take opposite roles contribute with their normalized weight negatively if $u \in H(e)$ and $v \in T(e)$ and positively if $u \in T(e)$ and $v \in H(e)$. Due to this, the imaginary part, $\Im((\vec{L}_N)_{uv})$, is affected by the *net*

contribution of u and v across all the directed hyperedges that contain them. This is in line with the *net flow* behavior observed by (Fiorini et al., 2023) for L^σ for the case of directed graphs. An example illustrating the construction of \vec{L}_N for a directed hypergraph is provided in Appendix F.

The relationship between \vec{L}_N and the previously-proposed Laplacian matrices that we introduced in Section 2 as well as its spectral properties are analyzed in more detail in what follows.

On the Relationship between \vec{L}_N and other Laplacian Matrices

The following theorem shows that \vec{L}_N and \vec{Q}_N generalize the Laplacian matrices proposed by Zhou et al. (2006) for undirected hypergraphs which are defined in equation 3 and equation 6:

Theorem 1. *If \mathcal{H} is an undirected hypergraph, $\vec{L}_N = \Delta$ and $\vec{Q}_N = Q_N$.*

Focusing on 2-uniform hypergraphs, we show that \vec{L}_N and \vec{Q}_N generalize the Signed and Signless Laplacian matrices L_N and Q_N defined in equation 3 and equation 4, which are classically used for undirected graphs (Chung and Graham, 1997):

Corollary 1. *If \mathcal{H} is an undirected 2-uniform hypergraph, $\vec{L}_N = \frac{1}{2}L_N$ and $\vec{Q}_N = \frac{1}{2}Q_N$.*

Focusing on the case of directed graphs, we establish under which conditions \vec{L}_N generalizes the Signum-Magnetic Laplacian proposed by Fiorini et al. (2023) and the Magnetic Laplacian introduced by Lieb and Loss (1993):

Theorem 2. *If \mathcal{H} is a directed 2-uniform hypergraph with no antiparallel edges, we have $\vec{L}_N = \frac{1}{2}L_N^\sigma$ with $A_s = A + A^\top$.*

Corollary 2. *If \mathcal{H} is a directed 2-uniform unweighted hypergraph with no antiparallel edges, we have $\vec{L}_N = \frac{1}{2}L_N^{(q)}$ with $q = \frac{1}{4}$ and $A_s = A + A^\top$.*

Key Spectral Properties of \vec{L}_N

We start by showing that \vec{L}_N and \vec{Q}_N admit an eigenvalue decomposition with real eigenvalues. The result is structural and follows after showing that both matrices are Hermitian:

Theorem 3. *\vec{L}_N and \vec{Q}_N are diagonalizable with real eigenvalues.*

Next, we show that the spectrum of \vec{Q}_N is nonnegative. This result is obtained by showing that \vec{Q}_N can be decomposed as the product of the matrix $D_v^{-\frac{1}{2}}\vec{B}W^{\frac{1}{2}}D_e^{-\frac{1}{2}}$ and its conjugate transpose:

Theorem 4. *\vec{Q}_N is positive semidefinite.*

To show that \vec{L}_N is positive semidefinite, we first derive the equation of $\|x\|_{\vec{L}_N}^2$, i.e. the p -Dirichlet energy function with $p = 2$ induced by the Generalized Directed Laplacian for a signal $x \in \mathbb{C}^n$. In line with the 2-uniform case (Shuman et al., 2013), such a function provides a measure of global smoothness for x across the entire hypergraph.

Theorem 5. *Let $x = a + ib \in \mathbb{C}^n$, with $a, b \in \mathbb{R}^n$. The 2-Dirichlet energy function $\|x\|_{\vec{L}_N}^2 = x^*\vec{L}_N x$ of x induced by \vec{L}_N is the following quadratic form:*

$$\begin{aligned} \frac{1}{2} \sum_{e \in E} \frac{w(e)}{\delta(e)} \sum_{u,v \in E} & \left(\left(\left(\frac{a_u}{\sqrt{d_u}} - \frac{a_v}{\sqrt{d_v}} \right)^2 + \left(\frac{b_u}{\sqrt{d_u}} - \frac{b_v}{\sqrt{d_v}} \right)^2 \right) \mathbf{1}_{u,v \in H(e) \vee u,v \in T(e)} \right. \\ & + \left(\left(\frac{a_u}{\sqrt{d_u}} + \frac{b_v}{\sqrt{d_v}} \right)^2 + \left(\frac{a_v}{\sqrt{d_v}} - \frac{b_u}{\sqrt{d_u}} \right)^2 \right) \mathbf{1}_{u \in H(e), v \in T(e)} \\ & \left. + \left(\left(\frac{a_u}{\sqrt{d_u}} - \frac{b_v}{\sqrt{d_v}} \right)^2 + \left(\frac{a_v}{\sqrt{d_v}} + \frac{b_u}{\sqrt{d_u}} \right)^2 \right) \mathbf{1}_{v \in H(e), u \in T(e)} \right), \end{aligned} \quad (10)$$

where $\mathbf{1}$ is the indicator function.

Corollary 3. \vec{L}_N is positive semidefinite.

The nonnegativity of the spectra of \vec{L}_N and \vec{Q}_N is an important property, as it shows that their eigenvalues can be naturally interpreted as graph frequencies, which is in line with the case of the Laplacian matrices of Section 2 defined for undirected hypergraphs and directed graphs.

Lastly, we combine Theorems 3 and 4 to derive upper bounds on the spectra of \vec{L}_N and \vec{Q}_N :

Corollary 4. $\lambda_{\max}(\vec{L}_N) \leq 1$ and $\lambda_{\max}(\vec{Q}_N) \leq 1$.

While these spectral bounds are not required for the construction of the convolution operator defined in equation 1, they are necessary to construct localized filters using Chebyshev’s polynomials of degree $K > 1$ (Kipf and Welling, 2017; Defferrard et al., 2016; He et al., 2022a), and could be of independent interest.

The proofs of the theorems and corollaries of this section can be found in Appendix B.

4 Generalized Directed Hypergraph Neural Network (GeDi-HNN)

We embed the Generalized Directed Laplacian \vec{L}_N in GeDi-HNN, the first HNN capable of handling hypergraphs with both undirected and directed edges via a spectral-based convolution operator. For this purpose, we rely on the localized filter of Section 2 which led to equation 1. Letting $\mathcal{L} = \vec{L}_N$, our convolution operator is $\hat{Y}x = \theta_0 I + \theta_1 \vec{L}_N$.

The adoption of a localized filter with two parameters θ_0, θ_1 plays an important role towards the generality and the flexibility of GeDi-HNN, which we highlight next:

Proposition 1. *The convolution operator obtained from equation 1 by letting $\mathcal{L} = \vec{L}_N$ with parameters θ_0, θ_1 coincides with the one obtained by letting $\mathcal{L} = \vec{Q}_N$ with parameters $\theta'_0 = \theta_0 + \theta_1, \theta'_1 = -\theta_1$.*

The proposition implies that GeDi-HNN generalizes previously-proposed GNNs and HNNs irrespective of whether they are designed around a Signed or a Signless Laplacian matrix (provided that either \vec{L}_N or \vec{Q}_N generalize the matrix such networks employ). This is because, as the proposition shows, GeDi-HNN can implement the convolution of equation 1 built on top of either Laplacians by learning suitable values for θ_0, θ_1 .

In our implementation, GeDi-HNN features the following extension of the convolution operator of equation 1. Let $X \in \mathbb{C}^{n \times c_0}$ be a c_0 -dimensional graph signal (a graph signal with c_0 input channels), which we compactly represent as a matrix. We combine θ_0 and θ_1 with the *mixing* operator that is commonly applied to X to linearly combine the c_0 channels of the graph signal. In doing so, we introduce two linear operators $\Theta_0, \Theta_1 \in \mathbb{C}^{c_0 \times c}$ which can either upscale (if $c > c_0$) or downscale (if $c < c_0$) the number of channels of X . A similar choice is made in other GNN/HNNs such as MagNet (Zhang et al., 2021b).

Letting ϕ be an activation function applied component-wise to its input matrix, the output $Z \in \mathbb{C}^{n \times c'}$ of one of GeDi-HNN’s convolutional layers is:

$$Z(X) = \phi \left(IX\Theta_0 + \vec{L}_N X\Theta_1 \right). \tag{11}$$

As activation function, we adopt a complex extension of the *ReLU* function, in which, for a given $z \in \mathbb{C}$, $\phi(z) = z$ if $\Re(z) \geq 0$ and $\phi(z) = 0$ otherwise. A similar choice is followed in other GNNs/HNNs works such as (Fiorini et al., 2023; 2024). We project the complex-valued output of the last convolutional layer into the reals via an *unwind* operation by which $Z(X) \in \mathbb{C}^{n \times c}$ is transformed into $(\Re(Z(X)) || \Im(Z(X))) \in \mathbb{R}^{n \times 2c}$, where $||$ is the concatenation operator.

To obtain the final result, we add ℓ linear layers to GeDi-HNN’s architecture and a residual connection for every convolutional layer except for the first one. These connections have been proven to aid in training deeper models by allowing them to retain information from the input of the previous layers (He et al., 2016; Kipf and Welling, 2017). GeDi-HNN’s architecture is depicted in Figure 1.

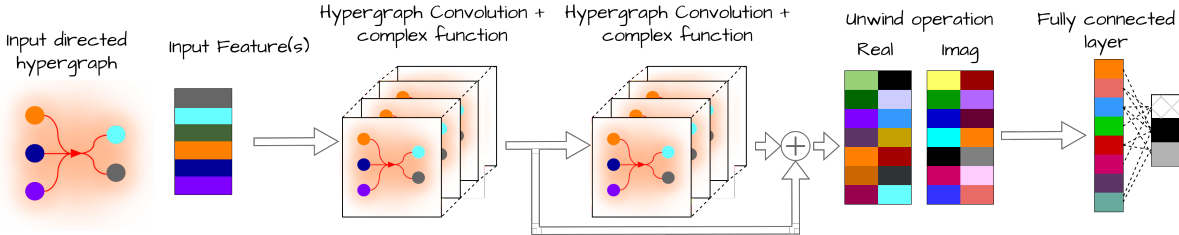


Figure 1: GeDi-HNN’s architecture: after two complex convolutional layers and a residual connection, we unwind the real and imaginary parts of the feature matrix and apply a fully connected layer.

Complexity of GeDi-HNN. Let us assume w.l.o.g. (as it does not affect the asymptotic analysis of complexity) that the input and output data of each convolutional layer except for the last one have c channels and that the output of the last convolutional layer and the number of channels of each linear layer are equal to c' . With ℓ convolutional layers and S linear layers, GeDi-HNN’s complexity is $O(\ell(n^2c + nc^2) + nc + (S - 1)(nc'^2) + nc'd + nd)$, where d is the number of hidden node classes (the last channel of the last linear layer). Letting $\bar{c} := \max\{c, c', d\}$ be the largest number of channels throughout the network, we have a complexity of $O(\ell(n^2\bar{c}) + (\ell + S)(n\bar{c}^2))$. Such a quantity is quadratic w.r.t. the number of nodes n and the largest number of channels \bar{c} , which is in line with previous GNNs and HNNs architectures. For more details see Appendix C.

5 Numerical Experiments

We now illustrate the results of an extensive set of experiments carried out to evaluate the performance of GeDi-HNN on directed hypergraphs. We compare our proposal against 11 state-of-the-art methods from the hypergraph-learning literature: HGNN (Feng et al., 2019), HCHA⁴ (Bai et al., 2021), HCHA with the attention mechanism (Bai et al., 2021), HNHN (Dong et al., 2020), HyperGCN (Yadati et al., 2019), UniGCNII (Huang and Yang, 2021), HyperDN (Tudisco et al., 2021), AllDeepSets (Chien et al., 2021), AllSetTransformer (Chien et al., 2021), LEGCN Yang et al. (2022), ED-HNN (Wang et al., 2023a), and PhenomNN (Wang et al., 2023b). The hyperparameters of these baselines and of our proposed model are selected via grid search (see Appendix E).

The experiments are carried out on the node classification task of predicting the class associated with each node, which is the same task that was consistently used throughout the papers where the 11 baselines were proposed. The comparison is carried out on real-world datasets (Subsection 5.1) and on synthetic hypergraphs (Subsection 5.2).

Throughout the following tables, the best results are reported in **boldface** and the second-best are underlined. The datasets and code we used are publicly available on GitHub (see Appendix A).

5.1 Node Classification Task on Real-World Datasets

We test GeDi-HNN on 10 real-world datasets from the literature: **Cora**, **Citeseer**, and **PubMed** (Zhang et al., 2022); **email-Enron** and **email-Eu** (Benson et al., 2018); **Texas**, **Wisconsin**, and **Cornell** (Pei et al., 2020); **WikiCS** (Mernyei and Cangea, 2020); and **Telegram** (Bovet and Grindrod, 2020). We test the 11 baselines (which, we recall, are not designed to handle directed hypergraphs) on an undirected version of the 10 datasets which is compiled following the procedure of (Feng et al., 2019). Differently, we test GeDi-HNN, which is the only method designed to handle directed hypergraphs, on a directed version of these instances, which we compile following a slight modification to the previous procedure. For every node p sharing a relationship with nodes a, b, c, d , we create the hyperedge e with $H(e) = \{p\}$ and $T(e) = \{a, b, c, d\}$. Considering, e.g., a citation relationship in **CiteSeer** where paper p cites papers a, b, c, d , in the undirected case we follow (Feng et al., 2019) and create the hyperedge $\{a, b, c, d\}$ to semantically represent the paper p whereas, in the directed case, we set $\{p\}$ as head and $\{a, b, c, d\}$ as tail. We adopt the split proposed by Zhang et al. (2021b) for **Telegram**,

⁴Among the many versions of HCHA in Dong et al. (2020), we use the one implemented in <https://github.com/Graph-COM/ED-HNN>, which coincides with HGNN⁺ (Gao et al., 2022).

Texas, Wisconsin, and Cornell and the split of Chien et al. (2021) on the other ones. All the experiments are conducted using 10-fold cross-validation. More details on the datasets can be found in Appendix D.

Table 1: Mean accuracy and standard deviation obtained on the node classification task on the real-world datasets. The results of Cora, Citeseer, and PubMed are taken from Table 3 of (Wang et al., 2023b).

Method	Cora	Citeseer	Pubmed	email-Eu	email-Enron
HGNN	79.39 ± 1.36	72.45 ± 1.16	86.44 ± 0.44	39.80 ± 2.77	44.32 ± 5.44
HCHA/HGNN ⁺	79.14 ± 1.02	72.42 ± 1.42	86.41 ± 0.36	41.01 ± 3.55	44.59 ± 6.77
HCHA w/ Attention	58.20 ± 2.53	68.44 ± 1.27	79.90 ± 1.70	28.75 ± 2.82	35.68 ± 6.96
HNHN	76.36 ± 1.92	72.64 ± 1.57	86.90 ± 0.30	29.92 ± 1.88	30.01 ± 12.56
HyperGCN	78.45 ± 1.26	71.28 ± 0.82	82.84 ± 8.67	30.81 ± 2.80	36.76 ± 5.87
UniGCNII	78.81 ± 1.05	73.05 ± 2.21	88.25 ± 0.40	40.81 ± 2.76	41.62 ± 5.28
LEGCN	74.74 ± 1.25	72.74 ± 0.86	88.12 ± 0.74	30.16 ± 2.28	35.41 ± 5.76
HyperND	79.20 ± 1.14	72.62 ± 1.49	86.68 ± 0.43	29.23 ± 1.80	35.41 ± 5.62
AllDeepSets	76.88 ± 1.80	70.83 ± 1.63	88.75 ± 0.33	29.92 ± 1.88	36.76 ± 7.01
AllSetTransformer	78.58 ± 1.47	73.08 ± 1.20	88.72 ± 0.37	41.58 ± 5.13	45.41 ± 8.43
ED-HNN	80.31 ± 1.35	73.70 ± 1.38	89.03 ± 0.53	30.85 ± 2.87	42.97 ± 7.37
PhenomNN	82.29 ± 1.42	75.10 ± 1.59	88.07 ± 0.48	31.09 ± 3.83	37.03 ± 7.21
GeDi-HNN	84.04 ± 1.15	75.68 ± 1.04	89.80 ± 0.51	49.27 ± 3.17	52.43 ± 5.28
GeDi-HNN w/o directions	78.85 ± 1.75	74.08 ± 1.15	88.67 ± 0.58	46.88 ± 3.04	48.38 ± 6.55

Method	Telegram	Texas	Wisconsin	Cornell	WikiCS
HGNN	59.42 ± 6.04	71.08 ± 7.32	75.69 ± 4.64	70.81 ± 4.73	77.95 ± 5.69
HCHA/HGNN ⁺	52.12 ± 3.32	71.35 ± 6.77	73.53 ± 5.41	70.81 ± 5.06	76.50 ± 5.07
HCHA w/ attention	57.69 ± 2.86	72.97 ± 6.50	70.59 ± 6.40	73.51 ± 4.73	11.67 ± 4.79
HNHN	50.77 ± 8.27	75.41 ± 7.26	81.18 ± 3.72	74.32 ± 5.14	26.47 ± 18.1
HyperGCN	55.77 ± 3.95	65.95 ± 9.03	70.98 ± 5.05	68.39 ± 6.87	75.80 ± 6.16
UniGCNII	55.58 ± 5.01	84.17 ± 5.44	86.47 ± 5.02	76.76 ± 5.13	83.24 ± 1.07
LEGCN	45.19 ± 5.15	79.19 ± 4.78	84.51 ± 5.35	73.78 ± 6.12	78.73 ± 1.19
HyperND	43.65 ± 4.35	81.62 ± 6.60	85.10 ± 4.45	74.87 ± 4.60	72.28 ± 3.14
AllDeepSets	38.46 ± 6.08	82.97 ± 5.85	84.51 ± 5.43	78.11 ± 3.70	83.00 ± 1.10
AllSetTransformer	57.12 ± 5.21	80.27 ± 5.56	81.96 ± 6.26	76.47 ± 5.41	83.37 ± 3.77
ED-HNN	54.42 ± 6.01	83.78 ± 7.64	86.27 ± 2.45	77.84 ± 5.67	82.12 ± 1.57
PhenomNN	54.61 ± 4.72	84.59 ± 5.41	86.28 ± 4.62	76.49 ± 5.56	80.07 ± 0.61
GeDi-HNN	75.01 ± 4.96	84.59 ± 4.78	88.43 ± 3.31	80.54 ± 2.79	82.23 ± 1.47
GeDi-HNN w/o directions	64.80 ± 6.60	83.51 ± 4.51	86.66 ± 4.96	77.83 ± 4.65	82.52 ± 1.19

The accuracy obtained across the different methods and datasets is reported in Table 1. The results show that, across the whole testbed, GeDi-HNN achieves an average additive performance improvement over the best-performing competitor of approximately 4.20 percentage points. In terms of Relative Percentage Difference (RPD)⁵, we have an average RPD improvement of 7.06%. The most significant improvement is observed for Telegram, where GeDi-HNN achieves an average RPD improvement of approximately 23.19% and an average additive improvement of 15.59 percentage points w.r.t. the best competitor from the literature (HGNN). Overall, GeDi-HNN ranks first on 9 out of 10 datasets and fourth on the 10th dataset, where it achieves an accuracy of 82.23, which is only 1.14 percentage points less than the best one recorded for the experiment.

Table 1 also presents the results of an ablation study aimed at demonstrating that a significant portion of the superior performance of GeDi-HNN is attributable to the Generalized Directed Laplacian \bar{L}_N rather than to the network’s architecture. In this study, we compare GeDi-HNN to GeDi-HNN w/o directions, a version which employs the undirected hypergraph Laplacian Δ proposed in Zhou et al. (2006) (which disregards hyperedge directions) instead of \bar{L}_N . As shown in Table 1, GeDi-HNN outperforms GeDi-HNN w/o directions with an RPD improvement of 4.90% (an additive difference of 3.35 percentage points) on average across 9 out of 10 datasets and achieves nearly identical performance on the 10th dataset (WikiCS), where the difference between the two versions is negligible (of, additively, only 0.29 percentage points). The largest improvement, observed on Telegram, is of a RPD of 14.61% (an additive difference of 10.21 percentage points).

These results underscore the importance of incorporating the directionality of the hyperedges and suggest that, thanks to the Generalized Directed Laplacian, GeDi-HNN effectively captures and utilizes this information.

⁵The RPD of two values P_1, P_2 is the percentage ratio of their difference to their average, i.e., $|P_1 - P_2| / \frac{P_1 + P_2}{2}$ %.

5.2 Node Classification Task on Synthetic Datasets

To emphasize the importance of leveraging the hypergraph’s directions in identifying the class of each node, we conduct a set of experiments on synthetic datasets specifically designed to exhibit a high degree of correlation between node classes and hyperedge directions.

Drawing inspiration from the methodology proposed in Zhang et al. (2021b), we rely on a collection of datasets which are generated as follows. First, the set V of vertices is partitioned into c equally-sized classes C_1, \dots, C_c with uniform probability. Subsequently, for each class C , I_i intra-class undirected hyperedges are created, each with a cardinality uniformly sampled from $\{h_{\min}, \dots, h_{\max}\}$, containing vertices of the same class, also sampled with uniform probability. Similarly, for each pair of classes C_i and C_j with $i < j$, I_o inter-class directed hyperedges are created. The head and tail sets are sampled from C_i and C_j , respectively, with uniform probability, and both have a cardinality uniformly sampled from $\{h_{\min}, \dots, h_{\max}\}$. Figure 2 portrays the directional flow that the hyperedges induce among the classes of a synthetic dataset with 5 classes. Notice how the flow is directed from a class C_i to a class C_j only if $i < j$.

Using this methodology, we generate three distinct datasets with the parameters $n = 500$, $c = 5$, $h_{\min} = 3$, $h_{\max} = 10$, $I_i = 30$, and an increasing number of inter-class hyperedges $I_o = 10, 30, 50$. For these datasets, we implement a 50%/25%/25% split for training, validation, and testing, respectively. The experiments are conducted using 10-fold cross-validation.

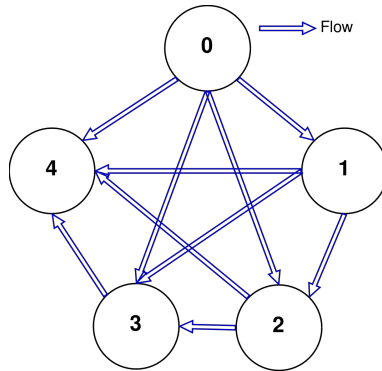


Figure 2: Schematic representation of the direction of the flow induced by the hyperedges in a synthetic dataset with 5 classes ($c = 5$).

Table 2: Mean accuracy and standard deviation obtained on the node classification tasks on the synthetic datasets.

Method	$I_o = 10$	$I_o = 30$	$I_o = 50$
HGNN	30.02 \pm 5.99	31.52 \pm 4.20	32.40 \pm 3.36
HCHA/HGNN ⁺	33.60 \pm 4.76	36.96 \pm 4.60	39.04 \pm 2.66
HCHA w/ Attention	17.28 \pm 2.42	18.64 \pm 2.64	20.44 \pm 2.24
HNN	19.28 \pm 4.16	20.16 \pm 3.88	19.28 \pm 2.86
HyperGCN	21.04 \pm 3.99	21.28 \pm 3.11	17.84 \pm 3.33
UniGCNII	20.80 \pm 3.94	21.52 \pm 3.72	20.40 \pm 4.67
LEGCN	17.84 \pm 1.31	19.76 \pm 5.27	19.84 \pm 4.04
HyperND	18.16 \pm 3.11	18.40 \pm 3.85	18.16 \pm 4.06
AllDeepSets	18.32 \pm 4.12	19.20 \pm 4.33	18.72 \pm 4.40
AllSet Transformer	19.44 \pm 4.42	18.96 \pm 4.30	22.72 \pm 5.06
ED-HNN	19.12 \pm 3.32	21.12 \pm 3.56	18.96 \pm 3.33
PhenomNN	20.88 \pm 4.24	21.20 \pm 4.30	20.32 \pm 4.62
GeDi-HNN	65.92 \pm 3.98	71.84 \pm 3.31	78.24 \pm 5.64
GeDi-HNN w/o directions	36.72 \pm 5.84	29.68 \pm 6.78	28.16 \pm 10.65

The experimental results, summarized in Table 2, indicate a substantial performance difference between GeDi-HNN and the other 11 baselines, which increases with higher values of I_o . On average, GeDi-HNN achieves an accuracy that surpasses the best competitor from the literature with an RPD improvement of 65.31% (an additive improvement of 35.47 percentage points). The additive difference compared to the second-best performer is of up to 39.19 percentage points.

We conclude with the ablation study where GeDi-HNN is compared to GeDi-HNN w/o directions. The results reveals a substantial accuracy difference of 40.48 percentage points (on average) between GeDi-HNN and GeDi-HNN w/o directions. Notably, as the number of inter-class hyperedges (I_o) increases, the performance of GeDi-HNN improves, while that of GeDi-HNN w/o directions declines. This finding

underscores the significant contribution of our proposed Generalized Directed Laplacian to the superior performance of GeDi-HNN.

6 Conclusion

We introduced GeDi-HNN, the first spectral HNN capable of handling hypergraphs with both undirected and directed edges. GeDi-HNN is built upon a novel complex-valued Laplacian matrix, the *Generalized Directed Laplacian*, which is a Hermitian matrix that employs a complex-number representation of the hyperedge directions. This approach naturally generalizes several previously proposed Laplacians for both graphs and hypergraphs. Our proposal enables the seamless integration of directionality in HNNs, which is crucial for accurately modeling various real-world phenomena involving asymmetric high-order interactions. Our proposed GeDi-HNN model utilizes this new Laplacian matrix to perform spectral convolutions on hypergraphs featuring both undirected and directed hyperedges.

Extensive computational experiments on both real-world and synthetic datasets have demonstrated the superior performance of GeDi-HNN in 12 out of 13 experiments compared to a comprehensive representative group of state-of-the-art methods for the node classification task. These findings underscore the importance of incorporating directional information within GeDi-HNN’s convolution operator. Specifically, GeDi-HNN consistently outperforms existing models across various datasets, achieving an average relative-percentage-difference improvement of 7% on real-world dataset (with a maximum improvement of 23.19%) and of 65.3% on synthetic datasets. The superiority of our method is particularly evident in the experiments on synthetic hypergraphs. These results highlight the potential of adopting GeDi-HNN to significantly enhance the modeling of complex, directed interactions within a hypergraph to the benefit of the hypergraph-learning task at hand.

Broader Impact Statement

All the data we used are publicly available for research purposes and do not contain personally identifiable information or offensive content (see Appendix A for more details). The methods presented here have an impact on society comparable to other graph neural network algorithms.

References

- Song Bai, Feihu Zhang, and Philip HS Torr. Hypergraph convolution and hypergraph attention. *Pattern Recognition*, 110:107637, 2021.
- Austin R. Benson, Rediet Abebe, Michael T. Schaub, Ali Jadbabaie, and Jon Kleinberg. Simplicial closure and higher-order link prediction. *Proceedings of the National Academy of Sciences*, 2018. ISSN 0027-8424. doi: 10.1073/pnas.1800683115.
- Alexandre Bovet and Peter Grindrod. The activity of the far right on Telegram. *ResearchGate preprint*, DOI: 10.13140/RG.2.2.16700.05764:1–19, 2020.
- Eli Chien, Chao Pan, Jianhao Peng, and Olgica Milenkovic. You are allset: A multiset function framework for hypergraph neural networks. In *International Conference on Learning Representations*, 2021.
- Fan RK Chung and Fan Chung Graham. *Spectral graph theory*. Number 92. American Mathematical Soc., 1997.
- Michaël Defferrard, Xavier Bresson, and Pierre Vandergheynst. Convolutional neural networks on graphs with fast localized spectral filtering. *Advances in neural information processing systems*, 29, 2016.
- Yihe Dong, Will Sawin, and Yoshua Bengio. Hnhn: Hypergraph networks with hyperedge neurons. *arXiv preprint arXiv:2006.12278*, 2020.
- Yifan Feng, Haoxuan You, Zizhao Zhang, Rongrong Ji, and Yue Gao. Hypergraph neural networks. In *Proceedings of the AAAI conference on artificial intelligence*, pages 3558–3565, 2019.

- Stefano Fiorini, Stefano Coniglio, Michele Ciavotta, and Enza Messina. Sigmanet: One laplacian to rule them all. In *Proceedings of the AAAI Conference on Artificial Intelligence*, pages 7568–7576, 2023.
- Stefano Fiorini, Stefano Coniglio, Michele Ciavotta, and Enza Messina. Graph learning in 4d: A quaternion-valued laplacian to enhance spectral gens. In *Proceedings of the AAAI Conference on Artificial Intelligence*, volume 38, pages 12006–12015, 2024.
- Giorgio Gallo, Giustino Longo, Stefano Pallottino, and Sang Nguyen. Directed hypergraphs and applications. *Discrete applied mathematics*, 42(2-3):177–201, 1993.
- Yue Gao, Yifan Feng, Shuyi Ji, and Rongrong Ji. Hgmn+: General hypergraph neural networks. *IEEE Transactions on Pattern Analysis and Machine Intelligence*, 45(3):3181–3199, 2022.
- David K Hammond, Pierre Vandergheynst, and Rémi Gribonval. Wavelets on graphs via spectral graph theory. *Applied and Computational Harmonic Analysis*, 30(2):129–150, 2011.
- Kaiming He, Xiangyu Zhang, Shaoqing Ren, and Jian Sun. Deep residual learning for image recognition. In *Proceedings of the IEEE conference on computer vision and pattern recognition*, pages 770–778, 2016.
- Mingguo He, Zhewei Wei, and Ji-Rong Wen. Convolutional neural networks on graphs with chebyshev approximation, revisited. *Advances in neural information processing systems*, 35:7264–7276, 2022a.
- Yixuan He, Xitong Zhang, Junjie Huang, Benedek Rozemberczki, Mihai Cucuringu, and Gesine Reinert. PyTorch Geometric Signed Directed: A Software Package on Graph Neural Networks for Signed and Directed Graphs. *arXiv preprint arXiv:2202.10793*, 2022b.
- Jing Huang and Jie Yang. Unigmn: a unified framework for graph and hypergraph neural networks. In *Proceedings of the Thirtieth International Joint Conference on Artificial Intelligence, IJCAI-21*, 2021.
- Thomas N. Kipf and Max Welling. Semi-supervised classification with graph convolutional networks. In *5th International Conference on Learning Representations, ICLR 2017 - Conference Track Proceedings*, 2017.
- Bryan Klimt and Yiming Yang. Introducing the enron corpus. In *CEAS*, volume 45, pages 92–96, 2004.
- Valerio La Gatta, Vincenzo Moscato, Mirko Pennone, Marco Postiglione, and Giancarlo Sperli. Music recommendation via hypergraph embedding. *IEEE transactions on neural networks and learning systems*, 2022.
- Yujia Li, Richard Zemel, Marc Brockschmidt, and Daniel Tarlow. Gated graph sequence neural networks. In *Proceedings of ICLR’16*, April 2016.
- Elliott H Lieb and Michael Loss. Fluxes, Laplacians, and Kasteleyn’s theorem. In *Statistical Mechanics*, pages 457–483. Springer, 1993.
- Xiaoyi Luo, Jiaheng Peng, and Jun Liang. Directed hypergraph attention network for traffic forecasting. *IET Intelligent Transport Systems*, 16(1):85–98, 2022.
- Péter Mernyei and Cătălina Cangea. Wiki-cs: A wikipedia-based benchmark for graph neural networks. *arXiv preprint arXiv:2007.02901*, 2020.
- Alessio Micheli. Neural network for graphs: A contextual constructive approach. *IEEE Transactions on Neural Networks*, 20(3):498–511, 2009.
- Ashwin Paranjape, Austin R Benson, and Jure Leskovec. Motifs in temporal networks. In *Proceedings of the tenth ACM international conference on web search and data mining*, pages 601–610, 2017.
- Hongbin Pei, Bingzhe Wei, Kevin Chen-Chuan Chang, Yu Lei, and Bo Yang. Geom-gcn: Geometric graph convolutional networks. *arXiv preprint arXiv:2002.05287*, 2020.
- Jörg Reichardt and Stefan Bornholdt. Statistical mechanics of community detection. *Physical review E*, 74(1):016110, 2006.

- Franco Scarselli, Marco Gori, Ah Chung Tsoi, Markus Hagenbuchner, and Gabriele Monfardini. The graph neural network model. *IEEE Transactions on Neural Networks*, 20(1):61–80, 2009.
- Michael T Schaub, Yu Zhu, Jean-Baptiste Seby, T Mitchell Roddenberry, and Santiago Segarra. Signal processing on higher-order networks: Livin’ on the edge... and beyond. *Signal Processing*, 187:108149, 2021.
- David I Shuman, Sunil K Narang, Pascal Frossard, Antonio Ortega, and Pierre Vandergheynst. The emerging field of signal processing on graphs: Extending high-dimensional data analysis to networks and other irregular domains. *IEEE signal processing magazine*, 30(3):83–98, 2013.
- Rahul Singh and Yongxin Chen. Signed graph neural networks: A frequency perspective. *Transactions on Machine Learning Research*, 2022.
- Francesco Tudisco, Austin R Benson, and Konstantin Prokopchik. Nonlinear higher-order label spreading. In *Proceedings of the Web Conference 2021*, pages 2402–2413, 2021.
- Petar Veličković, Guillem Cucurull, Arantxa Casanova, Adriana Romero, Pietro Liò, and Yoshua Bengio. Graph attention networks. In *International Conference on Learning Representations*, 2018.
- Peihao Wang, Shenghao Yang, Yunyu Liu, Zhangyang Wang, and Pan Li. Equivariant hypergraph diffusion neural operators. In *International Conference on Learning Representations (ICLR)*, 2023a.
- Yuxin Wang, Quan Gan, Xipeng Qiu, Xuanjing Huang, and David Wipf. From hypergraph energy functions to hypergraph neural networks. In *Proceedings of the 40th International Conference on Machine Learning*, pages 35605–35623, 2023b.
- Naganand Yadati, Madhav Nimishakavi, Prateek Yadav, Vikram Nitin, Anand Louis, and Partha Talukdar. Hypergcn: A new method for training graph convolutional networks on hypergraphs. *Advances in neural information processing systems*, 32, 2019.
- Chaoqi Yang, Ruijie Wang, Shuochao Yao, and Tarek Abdelzaher. Semi-supervised hypergraph node classification on hypergraph line expansion. 2022.
- Jie Zhang, Bo Hui, Po-Wei Harn, Min-Te Sun, and Wei-Shinn Ku. smgc: A complex-valued graph convolutional network via magnetic laplacian for directed graphs, 2021a.
- Jiying Zhang, Fuyang Li, Xi Xiao, Tingyang Xu, Yu Rong, Junzhou Huang, and Yatao Bian. Hypergraph convolutional networks via equivalency between hypergraphs and undirected graphs. *arXiv preprint arXiv:2203.16939*, 2022.
- Xitong Zhang, Yixuan He, Nathan Brugnone, Michael Perlmutter, and Matthew Hirn. Magnet: A neural network for directed graphs, 2021b.
- Dengyong Zhou, Jiayuan Huang, and Bernhard Schölkopf. Learning with hypergraphs: Clustering, classification, and embedding. *Advances in neural information processing systems*, 19, 2006.

A Code Repository and Licensing

The code written for this research work is available at https://anonymous.4open.science/r/GD_HNN-A8C5 and freely distributed under the Apache 2.0 license.⁶

The Texas, Wisconsin, Cornell, WikiCS, and Telegram datasets were obtained from the PyTorch Geometric Signed Directed (He et al., 2022b) library (provided under the MIT license). The Cora, Citeseer, and PubMed datasets are available at <https://linqs.org/datasets/>. The email-Eu and email-Enron datasets are available at <https://www.cs.cornell.edu/~arb/data/>.

The code for the baselines used in the experimental analysis is available at <https://github.com/Graph-COM/ED-HNN> and <https://github.com/yxzwang/PhenomNN> under the MIT license.⁷

B Properties of Our Proposed Laplacian \vec{L}_N

This section contains the proofs of the theorems, corollaries, propositions, and lemmata reported in the main paper.

Theorem 1. *If \mathcal{H} is an undirected hypergraph, $\vec{L}_N = \Delta$ and $\vec{Q}_N = Q_N$.*

Proof. Since $\mathcal{H} = (V, E)$ is an undirected hypergraph, \vec{B} is binary and only takes values 0 and 1 (rather than being ternary and taking values $-0, 1, -1$). In particular, for each edge $e \in E$ we have $\vec{B}_{ue} = 1$ if either $u \in H(e)$ or $u \in T(e)$ and $\vec{B}_{ue} = 0$ otherwise. Consequently, the directed incident matrix \vec{B} is identical to the non-directed incidence matrix B , i.e., $\vec{B} = B$. Thus, by construction, $\vec{L}_N = \Delta$ and $\vec{Q}_N = Q_N$. \square

Corollary 1. *If \mathcal{H} is an undirected 2-uniform hypergraph, $\vec{L}_N = \frac{1}{2}L_N$ and $\vec{Q}_N = \frac{1}{2}Q_N$.*

Proof. Since \mathcal{H} is an undirected 2-uniform hypergraph, it follows that:

$$\begin{cases} \vec{B}W\vec{B}^* &= D_v + A \\ D_e^{-1} &= \frac{1}{2}I \end{cases}$$

Based on this, we can rewrite \vec{Q}_N as follows:

$$\begin{aligned} \vec{Q}_N &= D_v^{-\frac{1}{2}}\vec{B}W D_e^{-1}\vec{B}^* D_v^{-\frac{1}{2}} \\ &= D_v^{-\frac{1}{2}}\vec{B}\left(\frac{1}{2}W\right)\vec{B}^* D_v^{-\frac{1}{2}} \\ &= \frac{1}{2}\left(D_v^{-\frac{1}{2}}(D_v + A)D_v^{-\frac{1}{2}}\right) \\ &= \frac{1}{2}\left(I + D_v^{-\frac{1}{2}}AD_v^{-\frac{1}{2}}\right) \\ &= \frac{1}{2}(I + A_N) \\ &= \frac{1}{2}Q_N \end{aligned}$$

This proves the second part of the result. As $\vec{Q}_N = \frac{1}{2}Q_N$ and, due to equation 5, $\frac{1}{2}L_N = I - \frac{1}{2}Q_N$, it follows that $\frac{1}{2}L_N = I - \vec{Q}_N = \vec{L}_N$. \square

Theorem 2. *If \mathcal{H} is a directed 2-uniform hypergraph with no antiparallel edges, we have $\vec{L}_N = \frac{1}{2}L_N^\sigma$ with $A_s = A + A^\top$.*

⁶<https://www.apache.org/licenses/LICENSE-2.0>

⁷<https://choosealicense.com/licenses/mit/>

Proof. As \mathcal{H} is a directed 2-uniform hypergraph without antiparallel edges, it follows that:

$$\begin{cases} \vec{B}W\vec{B}^* &= \bar{D}_s + H^\sigma \\ D_e^{-1} &= \frac{1}{2}I. \end{cases}$$

$A_s = A + A^\top$ implies $\bar{D}_s = D_v$. Thus, we can rewrite \vec{L}_N :

$$\begin{aligned} \vec{L}_N &= I - D_v^{-\frac{1}{2}}\vec{B}W D_e^{-1}\vec{B}^* D_v^{-\frac{1}{2}} \\ &= I - D_v^{-\frac{1}{2}}\vec{B} \left(\frac{1}{2}W \right) \vec{B}^* D_v^{-\frac{1}{2}} \\ &= I - \frac{1}{2} \left(D_v^{-\frac{1}{2}} (\bar{D}_s + H^\sigma) D_v^{-\frac{1}{2}} \right) \\ &= I - \frac{1}{2} \left(I + D_v^{-\frac{1}{2}} H^\sigma D_v^{-\frac{1}{2}} \right) \\ &= \frac{1}{2} L_N^\sigma. \end{aligned}$$

□

Corollary 2. *If \mathcal{H} is a directed 2-uniform unweighted hypergraph with no antiparallel edges, we have $\vec{L}_N = \frac{1}{2}L_N^{(q)}$ with $q = \frac{1}{4}$ and $A_s = A + A^\top$.*

Proof. As \mathcal{H} is a directed 2-uniform unweighted hypergraph, $A \in \{0, 1\}^{n \times n}$. Thus, as shown by Fiorini et al. (2023), with $q = \frac{1}{4}$ we have $L^\sigma = L^{(q)}$. Since Theorem 2 states that $\vec{L}_N = \frac{1}{2}L_N^\sigma$, it follows that

$$\vec{L}_N = \frac{1}{2}L_N^\sigma = \frac{1}{2}L^{(\frac{1}{4})}.$$

□

Theorem 3. *\vec{L}_N and \vec{Q}_N are diagonalizable with real eigenvalues.*

Proof. This follows from the fact that the two matrices are, by construction, Hermitian. □

Theorem 4. *\vec{Q}_N is positive semidefinite.*

Proof.

$$\begin{aligned} x^* \vec{Q}_N x &:= x^* \left(D_v^{-\frac{1}{2}} \vec{B}W D_e^{-1} \vec{B}^* D_v^{-\frac{1}{2}} \right) x \\ &\quad \left(x^* D_v^{-\frac{1}{2}} \vec{B}W^{\frac{1}{2}} D_e^{-\frac{1}{2}} \right) \left(D_e^{-\frac{1}{2}} W^{\frac{1}{2}} \vec{B}^* D_v^{-\frac{1}{2}} x \right) \\ &\quad \left(D_e^{-\frac{1}{2}} W^{\frac{1}{2}} \vec{B}^* D_v^{-\frac{1}{2}} x \right)^* \left(D_e^{-\frac{1}{2}} \vec{B}^* W^{\frac{1}{2}} D_v^{-\frac{1}{2}} x \right) \\ &\quad \left\| \left(D_e^{-\frac{1}{2}} W^{\frac{1}{2}} \vec{B}^* D_v^{-\frac{1}{2}} x \right)^* \right\|_2^2 \geq 0. \end{aligned}$$

□

Theorem 5. *Let $x = a + ib \in \mathbb{C}^n$, with $a, b \in \mathbb{R}^n$. The 2-Dirichlet energy function $\|x\|_{\vec{L}_N}^2 = x^* \vec{L}_N x$ of x induced by \vec{L}_N is the following quadratic form:*

$$\begin{aligned} &\frac{1}{2} \sum_{e \in E} \frac{w(e)}{\delta(e)} \sum_{u, v \in E} \left(\left(\left(\frac{a_u}{\sqrt{d_u}} - \frac{a_v}{\sqrt{d_v}} \right)^2 + \left(\frac{b_u}{\sqrt{d_u}} - \frac{b_v}{\sqrt{d_v}} \right)^2 \right) \mathbf{1}_{u, v \in H(e) \vee u, v \in T(e)} \right. \\ &\quad + \left(\left(\frac{a_u}{\sqrt{d_u}} + \frac{b_v}{\sqrt{d_v}} \right)^2 + \left(\frac{a_v}{\sqrt{d_v}} - \frac{b_u}{\sqrt{d_u}} \right)^2 \right) \mathbf{1}_{u \in H(e), v \in T(e)} \\ &\quad \left. + \left(\left(\frac{a_u}{\sqrt{d_u}} - \frac{b_v}{\sqrt{d_v}} \right)^2 + \left(\frac{a_v}{\sqrt{d_v}} + \frac{b_u}{\sqrt{d_u}} \right)^2 \right) \mathbf{1}_{v \in H(e), u \in T(e)} \right), \end{aligned} \quad (12)$$

where $\mathbf{1}$ is the indicator function.

Proof.

$$\begin{aligned}
x^* \vec{L}_N x &= \sum_{u \in V} x_u^* x_u - \sum_{u, v \in V} \sum_{e \in E} \frac{w(e)}{\delta(e)} \frac{\bar{B}(u, e) \bar{B}(v, e)^*}{\sqrt{d(u)} \sqrt{d(v)}} x_u x_v^* \\
&= \sum_{u \in V} x_u^* x_u - \sum_{e \in E} \sum_{u, v \in V} \frac{w(e)}{\delta(e)} \frac{\bar{B}(u, e) \bar{B}(v, e)^*}{\sqrt{d(u)} \sqrt{d(v)}} x_u x_v^* \\
&= \sum_{u \in V} x_u^* x_u - \sum_{e \in E} \frac{w(e)}{\delta(e)} \sum_{u, v \in V: u \leq v} \left(\bar{B}(u, e) \bar{B}(v, e)^* \frac{x_u x_v^*}{\sqrt{d(u)} \sqrt{d(v)}} + \bar{B}(v, e) \bar{B}(u, e)^* \frac{x_v x_u^*}{\sqrt{d(v)} \sqrt{d(u)}} \right) \\
&= \sum_{e \in E} \frac{w(e)}{\delta(e)} \sum_{u, v \in E: u \leq v} \left(\frac{x_u^* x_u}{d(u)} + \frac{x_v^* x_v}{d(v)} \right) \\
&\quad - \sum_{e \in E} \frac{w(e)}{\delta(e)} \sum_{u, v \in V: u \leq v} \left(\bar{B}(u, e) \bar{B}(v, e)^* \frac{x_u x_v^*}{\sqrt{d(u)} \sqrt{d(v)}} + \bar{B}(v, e) \bar{B}(u, e)^* \frac{x_v x_u^*}{\sqrt{d(v)} \sqrt{d(u)}} \right) \\
&= \sum_{e \in E} \frac{w(e)}{\delta(e)} \sum_{u, v \in E: u \leq v} \left(\frac{x_u^* x_u}{d(u)} + \frac{x_v^* x_v}{d(v)} - \bar{B}(u, e) \bar{B}(v, e)^* \frac{x_u x_v^*}{\sqrt{d(u)} \sqrt{d(v)}} - \bar{B}(v, e) \bar{B}(u, e)^* \frac{x_v x_u^*}{\sqrt{d(v)} \sqrt{d(u)}} \right).
\end{aligned}$$

Let us analyze the three possible cases for the summand.

Case 1.a: $u \in H(e) \wedge v \in H(e) \Leftrightarrow \bar{B}(u, e) = 1, \bar{B}(v, e) = 1$. We have $\bar{B}(u, e) \bar{B}(v, e)^* = \bar{B}(v, e) \bar{B}(u, e)^* = 1$.

Case 1.b: $u \in T(e) \wedge v \in T(e) \Leftrightarrow \bar{B}(u, e) = -i, \bar{B}(v, e) = -i$. We have $\bar{B}(u, e) \bar{B}(v, e)^* = \bar{B}(v, e) \bar{B}(u, e)^* = (-i)(-i)^* = (-i)(i) = 1$.

In both cases, we have:

$$\frac{x_u^* x_u}{d(u)} + \frac{x_v^* x_v}{d(v)} - \frac{x_u x_v^*}{\sqrt{d(u)} \sqrt{d(v)}} - \frac{x_v x_u^*}{\sqrt{d(v)} \sqrt{d(u)}} = \left(\frac{x_u}{\sqrt{d(u)}} - \frac{x_v}{\sqrt{d(v)}} \right)^* \left(\frac{x_u}{\sqrt{d(u)}} - \frac{x_v}{\sqrt{d(v)}} \right).$$

Letting $x_u = a_u + ib_u$ and $x_v = a_v + ib_v$, we have:

$$\left(\frac{a_u}{\sqrt{d_u}} - \frac{a_v}{\sqrt{d_v}} \right)^2 + \left(\frac{b_u}{\sqrt{d_u}} - \frac{b_v}{\sqrt{d_v}} \right)^2.$$

Case 2.a: $u \in H(e) \wedge v \in T(e) \Leftrightarrow \bar{B}(u, e) = 1, \bar{B}(v, e) = -i$. We have $\bar{B}(u, e) \bar{B}(v, e)^* = (1)(-i)^* = i$ and $\bar{B}(v, e) \bar{B}(u, e)^* = (-i)(1)^* = -i$.

Thus:

$$\frac{x_u^* x_u}{d(u)} + \frac{x_v^* x_v}{d(v)} - i \frac{x_u x_v^*}{\sqrt{d(u)} \sqrt{d(v)}} + i \frac{x_v x_u^*}{\sqrt{d(v)} \sqrt{d(u)}}$$

Let $x_u = a_u + ib_u$ and $x_v = a_v + ib_v$, then we have:

$$\left(\frac{a_u}{\sqrt{d_u}} + \frac{b_v}{\sqrt{d_v}} \right)^2 + \left(\frac{a_v}{\sqrt{d_v}} - \frac{b_u}{\sqrt{d_u}} \right)^2.$$

Case 2.b: $u \in T(e) \wedge v \in H(e) \Leftrightarrow \bar{B}(u, e) = -i, \bar{B}(v, e) = 1$. We have $\bar{B}(u, e) \bar{B}(v, e)^* = (-i)(1)^* = -i$ and $\bar{B}(v, e) \bar{B}(u, e)^* = (1)(-i)^* = i$. We have:

$$\frac{x_u^* x_u}{d(u)} + \frac{x_v^* x_v}{d(v)} + i \frac{x_u x_v^*}{\sqrt{d(u)} \sqrt{d(v)}} - i \frac{x_v x_u^*}{\sqrt{d(v)} \sqrt{d(u)}}$$

Let $x_u = a_u + ib_u$ and $x_v = a_v + ib_v$, then we have:

$$\left(\frac{a_u}{\sqrt{d_u}} - \frac{b_v}{\sqrt{d_v}}\right)^2 + \left(\frac{a_v}{\sqrt{d_v}} + \frac{b_u}{\sqrt{d_u}}\right)^2.$$

The final equation reported in the statement of the theorem is obtained by combining the four cases we just analyzed. \square

Corollary 3. \vec{L}_N is positive semidefinite.

Proof. Since \vec{L}_N is Hermitian, it can be diagonalized as $U\Lambda U^*$ for some $U \in \mathbb{C}^{n \times n}$ and $\Lambda \in \mathbb{R}^{n \times n}$, where Λ is diagonal and real. We have $x^* \vec{L}_N x = x^* U \Lambda U^* x = y^* \Lambda y$ with $y = U^* x$. Since Λ is diagonal, we have $y^* \Lambda y = \sum_{u \in V} \lambda_u y_u^2$. Thanks to Theorem 5, the quadratic form $x^* \vec{L}_N x$ associated with \vec{L}_N is a sum of squares and, hence, nonnegative. Combined with $x^* \vec{L}_N x = \sum_{u \in V} \lambda_u y_u^2$, we deduce $\lambda_u \geq 0$ for all $u \in V$. \square

Corollary 4. $\lambda_{\max}(\vec{L}_N) \leq 1$ and $\lambda_{\max}(\vec{Q}_N) \leq 1$.

Proof. $\lambda_{\max}(\vec{L}_N) \leq 1$ holds if and only if $\vec{L}_N - I \preceq 0$. Since $\vec{L}_N = I - \vec{Q}_N$ holds by definition, we need to prove $-\vec{Q}_N \preceq 0$, which holds true due to Theorem 4.

Similarly, $\lambda_{\max}(\vec{Q}_N) \leq 1$ holds if and only if $\vec{Q}_N - I \preceq 0$. Since $\vec{Q}_N = I - \vec{L}_N$ holds by definition, we need to prove $-\vec{L}_N \preceq 0$, which holds true due to Theorem 3. \square

Proposition 1. The convolution operator obtained from equation 1 by letting $\mathcal{L} = \vec{L}_N$ with parameters θ_0, θ_1 coincides with the one obtained by letting $\mathcal{L} = \vec{Q}_N$ with parameters $\theta'_0 = \theta_0 + \theta_1, \theta'_1 = -\theta_1$.

Proof. Consider the two operators $\theta_0 I + \theta_1 \vec{L}_N$ and $\theta'_0 I + \theta'_1 \vec{Q}_N$. Since $\vec{L}_N = I - \vec{Q}_N$, the first operator reads: $\theta_0 I + \theta_1 (I - \vec{Q}_N)$. This is rewritten as $(\theta_0 + \theta_1) I - \theta_1 \vec{Q}_N$. By operating the choice $\theta'_0 = \theta_0 + \theta_1$ and $\theta'_1 = -\theta_1$, the second operator is obtained. \square

C Complexity of GeDi-HNN

The detailed calculations for the (inference) complexity of GeDi-HNN are as follows.

1. The Generalized Directed Laplacian \vec{L}_N is constructed following equation 7 in time $O(n^2 m)$, where the factor m is due to the need for computing the product between two rows of \vec{B} to calculate each entry of \vec{L}_N . After \vec{L}_N has been computed, the convolution matrix $\hat{Y} \in \mathbb{C}^{n \times n}$ is constructed in time $O(n^2)$. Note that such a construction is carried out entirely in pre-processing and is not required at inference time.
2. Each of the ℓ convolutional layers of GeDi-HNN requires $O(n^2 c + n c^2 + n c) = O(n^2 c + n c^2)$ elementary operations across 3 steps. Let X^{l-1} be the input matrix to layer $l = 1, \dots, \ell$. The operations that are carried out are the following ones.
 - (a) \vec{L}_N is multiplied by the node-feature matrix $X^{l-1} \in \mathbb{C}^{n \times c}$, obtaining $P^{l1} \in \mathbb{C}^{n \times c}$ in time $O(n^2 c)$ (we assume matrix multiplications takes cubic time);
 - (b) The matrices $P^{l0} = I X^{l-1} = X^{l-1}$ and P^{l1} are multiplied by the weight matrices $\Theta_0, \Theta_1 \in \mathbb{R}^{c \times c}$ (respectively), obtaining the intermediate matrices $P^{l01}, P^{l11} \in \mathbb{C}^{n \times c}$ in time $O(n c^2)$.
 - (c) The matrices P^{l01} and P^{l11} are added in time $O(n c)$ to obtain P^{l2} .
 - (d) The activation function ϕ is applied component wise to P^{l2} in time $O(n c)$, resulting in the output matrix $X^l \in \mathbb{C}^{n \times c}$ of the l -th convolutional layer.
3. The unwind operator transforms X^ℓ (the output of the last convolutional layer ℓ) into the matrix $U^0 \in \mathbb{R}^{n \times 2c}$ in linear time $O(n c)$.

4. Call U^{s-1} the input matrix to each linear layer of index $s = 1, \dots, S$. The application of the s -th linear layer to $U^{s-1} \in \mathbb{C}^{n \times c'}$ requires multiplying U^{s-1} by a weight matrix $M_s \in \mathbb{C}^{c' \times c'}$ (where c' is the number of channels from which and into which the feature vector of each node is projected). This is done in time $O(nc'^2)$.
5. In the last linear layer of index S , the input matrix $U^{S-1} \in \mathbb{R}^{n \times c'}$ is projected into the output matrix $O \in \mathbb{R}^{n \times d}$ in time $O(nc'd)$.
6. The application of the Softmax activation function takes linear time $O(nd)$.

We deduce an overall complexity of $O(\ell(n^2c + nc^2) + nc + (S - 1)(nc'^2) + nc'd + nd)$ which, letting $\bar{c} = \max\{c, c', d\}$, coincides with $O(\ell(n^2\bar{c}) + (\ell + S)(n\bar{c}^2))$.

D Further Details on the Datasets

We test GeDi-HNN on ten real-world dataset. **Cora**, **Citeseer**, and **PubMed** (Zhang et al., 2022); **email-Eu**, and **email-Enron** (Benson et al., 2018); **Texas**, **Wisconsin**, and **Cornell** (Pei et al., 2020); **WikiCS** (Mernyei and Cangea, 2020); and **Telegram** (Bovet and Grindrod, 2020).

Cora, **Citeseer**, and **PubMed** are citation networks with node labels based on paper topics. In these citation networks, the nodes represent papers, their relationships denote citations of one paper by another, and the node features are the bag-of-words representation of papers.

Email-Enron and **email-Eu** are two email datasets—one from communications exchanged between Enron employees (Klimt and Yang, 2004) and the other from a European research institution (Paranjape et al., 2017). The nodes are email addresses and their relationships are of sender-receiver type. Since no node labeling is present in these two datasets, we define the node labels (node classes) using the Spinglass algorithm (Reichardt and Bornholdt, 2006).

Texas, **Wisconsin**, and **Cornell** are WebKB data sets extracted from the CMU World Wide Knowledge Base (**Web->KB**) project.⁸ WebKB is a webpage data set collected from computer science departments of various universities by Carnegie Mellon University. In these networks, the nodes represent web pages, and the relationship are hyperlinks between them. The node features are the bag-of-words representation of the web pages. The web pages are manually classified into the five categories: student, project, course, staff, and faculty.

WikiCS is a directed network whose nodes correspond to Computer Science articles, and the relationships are on hyperlinks. This network has 10 classes representing different branches of the field.

Telegram models an influence network built on top of interactions among distinct users who propagate ideologies of a political nature.

The statistic of these ten real-world datasets and of the synthetic datasets we generate are summarized in Tables 3 and 4.

E Experiment Details

Hardware. The experiments were conducted on 2 different machines:

1. An Intel(R) Xeon(R) Gold 6326 CPU @ 2.90GHz with 380 GB RAM, equipped with an NVIDIA Ampere A100 40GB.
2. A 12th Gen Intel(R) Core(TM) i9-12900KF CPU @ 3.20GHz CPU with 64 GB RAM, equipped with an NVIDIA RTX 4090 GPU.

⁸<http://www.cs.cmu.edu/afs/cs.cmu.edu/project/theo-11/www/wwkb/>

Table 3: Statistics of the ten real-world datasets

Data set	# node	# hyperedges	# classes	average $ e $
Cora	2708	1579	7	3.03
Citeseer	3312	1079	6	3.20
Pubmed	19717	7963	3	4.35
email-Eu	986	873	10	38.01
email-Enron	143	128	7	20.03
Telegram	245	185	4	48.04
Texas	183	40	5	4.45
Wisconsin	251	65	5	4.77
Cornell	183	41	5	3.88
WikiCS	11701	6827	10	42.08

Table 4: Statistics of the synthetic datasets

Data set	# node	# hyperedges	# classes	average $ e $
$I_o = 10$	500	250	5	9.05
$I_o = 30$	500	450	5	10.79
$I_o = 50$	500	650	5	11.63

Model Settings. We trained every learning model considered in this paper for up to 500 epochs. We adopted a learning rate of $5 \cdot 10^{-3}$ and employed the optimization algorithm Adam with weight decays equal to $5 \cdot 10^{-4}$ (in order to avoid overfitting). For all the models that adopt the classification layer, we set it to 2.

We adopted a hyperparameter optimization procedure to identify the best set of parameters for each model. In particular, the hyperparameter values are:

- For AllDeepSets and ED-HNN, the number of basic block is chosen in $\{2, 4, 8\}$, the number of MLPs per block in $\{1, 2\}$, the dimension of the hidden MLP (i.e., the number of filters) in $\{64, 128, 256, 512\}$, and the classifier hidden dimension in $\{64, 128, 256\}$.
- For AllSetTransformer the number of basic block is chosen in $\{2, 4, 8\}$, the number of MLPs per block in $\{1, 2\}$, the dimension of the hidden MLP in $\{64, 128, 256, 512\}$, the classifier hidden dimension in $\{64, 128, 256\}$, and the number of heads in $\{1, 4, 8\}$.
- For UniGCNII, HGNN, HNHN, HCHA/HGNN⁺, LEGCN, and HCHA with the attention mechanism, the number of basic blocks is chosen in $\{2, 4, 8\}$ and the hidden dimension of the MLP layer in $\{64, 128, 256, 512\}$.
- For HyperGCN, the number of basic blocks is chosen in $\{2, 4, 8\}$.
- For HyperND, the classifier hidden dimension is chosen in $\{64, 128, 256\}$.
- For PhenomNN, the number of basic blocks is chosen in $\{2, 4, 8\}$. We select four different settings:
 1. $\lambda_0 = 0.1$, $\lambda_1 = 0.1$ and prop step= 8,
 2. $\lambda_0 = 0$, $\lambda_1 = 50$ and prop step= 16,
 3. $\lambda_0 = 1$, $\lambda_1 = 1$ and prop step= 16,
 4. $\lambda_0 = 0$, $\lambda_1 = 20$ and prop step= 16.
- For GeDi-HNN and GeDi-HNN w/o **directionality**, the number of convolutional layers is chosen in $\{1, 2, 3\}$, the number of filters in $\{64, 128, 256, 512\}$, and the classifier hidden dimension in $\{64, 128, 256\}$. We tested GeDi-HNN both with the input feature matrix $X \in \mathbb{C}^{n \times c}$ where $\Re(X) = \Im(X) \neq 0$ and with $\Im(X) = 0$.

Node Features. For Cora, Citeseer, PubMed, Texas, Wisconsin, Cornell, WikiCS, and Telegram, we retain the datasets' original features. For email-Eu, email-Enron, and the synthetic datasets, the feature vectors are generated using the vertex degree of each node.

F From a Directed Hypergraph to the Generalized Directed Laplacian

To illustrate the representation of a directed hypergraph in our Generalized Directed Laplacian, consider a directed hypergraph $\mathcal{H} = (V, E)$ with $V = \{v_1, v_2, v_3, v_4, v_5\}$ and $E = \{e_1, e_2\}$. The incidence relationships are defined as follows: $v_1, v_2 \in H(e_1)$, $v_3 \in T(e_1)$, $v_4, v_5 \in H(e_2)$, and $v_1, v_2 \in T(e_2)$. The hyperedges have unit weights (i.e., $W = I$). The hyperedge cardinalities are $\delta_{e_1} = 3$ and $\delta_{e_2} = 4$.

For this hypergraph, we construct our Generalized Directed Laplacian using the following matrices: the incidence matrix \vec{B} , its conjugate transpose \vec{B}^* , the vertex degree matrix D_v , and the hyperedge degree matrix D_e .

$$\vec{B} = \begin{bmatrix} 1 & i \\ 1 & i \\ -i & 0 \\ 0 & 1 \\ 0 & 1 \end{bmatrix} \quad \vec{B}^* = \begin{bmatrix} 1 & 1 & i & 0 & 0 \\ i & i & 0 & 1 & 1 \end{bmatrix} \quad D_v = \begin{bmatrix} 2 & 0 & 0 & 0 & 0 \\ 0 & 2 & 0 & 0 & 0 \\ 0 & 0 & 1 & 0 & 0 \\ 0 & 0 & 0 & 1 & 0 \\ 0 & 0 & 0 & 0 & 1 \end{bmatrix} \quad D_e = \begin{bmatrix} 3 & 0 \\ 0 & 4 \end{bmatrix}.$$

Based on these matrices, we build the \vec{Q}_N :

$$\vec{Q}_N = \begin{bmatrix} 0.29 & 0.29 & i0.24 & -i0.18 & -i0.18 \\ 0.29 & 0.29 & i0.24 & -i0.18 & -i0.18 \\ -i0.24 & -i0.24 & 0.33 & 0 & 0 \\ i0.18 & i0.18 & 0 & 0.25 & 0.25 \\ i0.18 & i0.18 & 0 & 0.25 & 0.25 \end{bmatrix}$$

and then our Generalized Directed Laplacian:

$$\vec{L}_N = \begin{bmatrix} 0.71 & -0.29 & -i0.24 & i0.18 & i0.18 \\ -0.29 & 0.71 & -i0.24 & i0.18 & i0.18 \\ i0.24 & i0.24 & 0.66 & 0 & 0 \\ -i0.18 & -i0.18 & 0 & 0.75 & -0.25 \\ -i0.18 & -i0.18 & 0 & -0.25 & 0.75 \end{bmatrix}$$

By inspecting \vec{L}_N , one can observe that it encodes the elements of the hypergraph in the following way:

1. The presence of nodes belonging to the same head or tail set, i.e., $v_1, v_2 \in H(e_1)$, $v_4, v_5 \in H(e_2)$, and $v_1, v_2 \in T(e_2)$, is encoded in the real part. Specifically, $(\vec{L}_N)_{v_1 v_2} = (\vec{L}_N)_{v_2 v_1} = -0.29$ and $(\vec{L}_N)_{v_4 v_5} = (\vec{L}_N)_{v_5 v_4} = -0.25$.
2. The directed hyperedges are encoded via the imaginary component. For example, considering nodes v_1 and v_3 , we have $(\vec{L}_N)_{v_1 v_3} = -(\vec{L}_N)_{v_3 v_1} = -i0.24$.
3. The absence of relationships between nodes is encoded by 0. Specifically, $(\vec{L}_N)_{v_3 v_4} = (\vec{L}_N)_{v_4 v_3} = 0$ and $(\vec{L}_N)_{v_3 v_5} = (\vec{L}_N)_{v_5 v_3} = 0$.
4. The "self-loop information" (a measure of how strongly the feature of a node depends on its current value within the convolution operator) is encoded by the diagonal of \vec{L}_N .

G Further insights on the relationship between $L^{(q)}$, L^σ , and \vec{L}_N .

We introduce the following modified version of the Magnetic Laplacian:

$$L'^{(q)} := D_s - H'^{(q)} \text{ and } L_N'^{(q)} := I - D_s^{-\frac{1}{2}} H'^{(q)} D_s^{-\frac{1}{2}},$$

where

$$H'^{(q)} := A_s \odot \exp \left(\sin(2\pi q (A - A^\top)) + i2 \cos(2\pi q (A - A^\top)) \right),$$

and the following modified version of the Sign-Magnetic Laplacian:

$$L'^\sigma := \bar{D}_s - H'^\sigma \text{ and } L_N'^\sigma := I - \bar{D}_s^{-\frac{1}{2}} H'^\sigma \bar{D}_s^{-\frac{1}{2}},$$

with

$$H'^\sigma := A_s \odot \left(ee^\top - \text{sgn}(|A - A^\top|) + i2 \text{sign}(|A| - |A^\top|) \right).$$

Both versions differ from their original definitions due to featuring an imaginary part which is twice as large. Such a modification is introduced to amend the asymmetric way in which vertex degrees and edge weights are accounted for in both Laplacians. Let us illustrate the rationale.

For undirected graphs, $A_{uv} = A_{vu} = 1$ signifies that the graph contains the edge $\{u, v\}$. Since $A_{s_{uv}} = A_{s_{vu}} = 1$, such an edge is correctly accounted for both in A_s and in the degree matrices D_s and \bar{D}_s (we recall that $D_s := \text{diag}(A_s e)$ and $\bar{D}_s := \text{diag}(|A_s| e)$).

For directed graphs, though, $A_{uv} = A_{vu} = 1$ signifies that the graph contains two directed edges (u, v) and (v, u) , rather than just one. In spite of this, in the original definitions of $L^{(q)}$ and L^σ we only have $A_{s_{uv}} = A_{s_{vu}} = 1$, which implies that only one of these edges is accounted for both in A_s and in the degree matrices D_v and \bar{D}_v . A similar issue arises when either $A_{uv} = 0$ (or $A_{vu} = 0$). In such a case, we have $A_{s_{uv}} = \frac{1}{2}$, implying that only half of the edge (u, v) (or (v, u)) is accounted for both in A_s and in D_v and \bar{D}_v .

In the modified versions of the two Laplacians, i.e., $L'^{(q)}$ and L'^σ , such an issue is amended thanks to upscaling by 2 the imaginary part of both matrices (which is the only part containing the information related to directed edges).

With these definitions, Theorem 2 and Corollary 2 can be extended as follows:

- If \mathcal{H} is a directed 2-uniform hypergraph, we have $\vec{L}_N = \frac{1}{2} L_N'^\sigma$.
- If \mathcal{H} is a directed 2-uniform unweighted hypergraph, then $\vec{L}_N = \frac{1}{2} L_N'^{(q)}$ with $q = \frac{1}{4}$.